

Perpendicular coupling to in-plane photonics using arc waveguides fabricated via two-photon polymerization

Chee-Wei Lee, Stefano Pagliara, Ulrich Keyser, and Jeremy J. Baumberg

Nanophotonics Centre, Cavendish Laboratory, University of Cambridge, Cambridge CB3 0HE, United Kingdom

(Received 20 March 2012; accepted 1 April 2012; published online 23 April 2012)

We demonstrate the concept of vertically standing arc waveguides to couple normally incident light into the plane of a photonic circuit or sensor array. The simple one-step direct write fabrication uses a low power picosecond microchip laser for two-photon polymerization with high-speed and low-cost. Arc waveguides with different arc radii and waveguide port diameters are obtained, with insertion loss down to 1.5 dB. This demonstration of a distinctly different architecture employing unsupported arc waveguides adds another dimension to photonic integration and opens up applications for environmental sensors, integrated microfluidics, bio-assay chips, as well as offering an alternate way of input/output-coupling to planar waveguides. © 2012 American Institute of Physics. [<http://dx.doi.org/10.1063/1.4704358>]

The rapid development of ultrashort lasers has enabled the precise localization of optical energy in time and space. This has spawned laser applications based on nonlinear optical interactions, such as two-photon polymerization, which enables fabrication of three-dimensional (3D) high resolution microstructures for various applications.^{1–5} This technique involves two-photon absorption in a photosensitive resist material which responds to the square of the incident light intensity and is subsequently polymerized. Non-illuminated regions of the photoresist are then washed away by developing in a solvent. Two-photon polymerization typically requires high threshold intensities, possible only with a tightly focussed short-pulse laser. By controlling the pulse energy and exposure time (or number of pulses), polymerization is initiated only at the focal point of the laser forming an oval-shaped voxel at each exposed point. These voxels are then cascaded three-dimensionally to construct a desired 3D structure by translating the focused laser spot. This allows 3D high-resolution resist structures to be formed in just one process step, in contrast with conventional one-photon lithography routes. Such structures can be used as the basis of a wide variety of 3D polymer optical waveguides, with advantages including cost effectiveness, low optical loss, rapid processibility, good environmental stability, and alignment to existing photonic, electronic or sensing structures.^{6,7}

In this paper, we report the production and characterization of vertical standing arc waveguides fabricated with two-photon polymerization using a picosecond microchip laser. Such arc waveguides have significant advantages in comparison with conventional sideways in-plane coupling to planar waveguides or integrated chips, since the input light can be coupled perpendicularly into the device from above or below the chip (Fig. 1(a)). This enables vertical coupling to waveguide arrays in a microscope configuration, combining large-field-of-view imaging with selected coupling to each channel. The ability to use vertical coupling was a key feature that revolutionised semiconductor lasers, allowing ridge lasers to be replaced by vertical-cavity designs and that led to ultra-low-cost high-density production and on-wafer testing. Vertical arc waveguides have cores which are sur-

rounded in all directions by air or liquid cladding and have low refractive index, so the evanescent wave is sensitive to environmental changes such as molecular binding. Arrays of arc waveguides can thus be used for environmental sensing, bio-assays, or similar planar devices (Fig. 1(b)).

The two-photon lithography system employs a sub-ns Nd:YAG microchip laser (TEEM Photonics) emitting 25 mW of 532 nm light in 550 ps pulses at 12 kHz repetition rate with a peak power of 3.5 kW. Compared to equivalent femtosecond lasers, this is a very compact economical design. The intensity-modulated laser module is coupled into an inverted microscope (Olympus) combined through a dichroic mirror and focussed onto the sample through an oil-immersion objective lens (Olympus 40 × NA 1.35). The sample is mounted on a 3D nano-positioning stage (Mad City Labs) attached to the microscope stage, allowing access to many individual fields of 200 × 200 μm². Computer control converts standard 3D design files into 3D exposures by synchronizing the laser and 3D stage with appropriate illumination intensities and exposure times for each voxel.

We utilize a commercial liquid photoresist, IP-L (Nanoscribe, Inc.), which is dedicated to two-photon absorption processing. This resist is drop-cast on top of a thin (170 μm-thick) glass substrate and the laser-induced crosslinking makes it insoluble in the iso-propyl alcohol developer (used with 20 min immersion), while the remaining regions are dissolved. Exposed regions also change in refractive index from 1.48 to 1.52 at visible wavelengths which thus allows real-time monitoring of the exposure process using CCD imaging

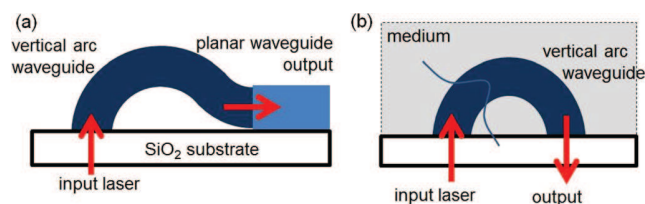


FIG. 1. Schematic design of vertical arc waveguides. (a) Vertical to in-plane light coupling to planar waveguide circuits. (b) Evanescent-wave sensors for bio- and environmental-sensing.

as well as directly inducing optical waveguiding. The vertical exposure height is limited by the working distance of the oil-immersion objective lens ($\sim 200\ \mu\text{m}$) and the substrate thickness, to less than $30\ \mu\text{m}$; however, this may be increased by using lower numerical aperture objectives. While direct writing through the transparent substrate is used here, the inverted configuration can also be adopted for opaque substrates.

Waveguides are characterized in an inverted microscope using the scheme in Fig. 1(b), with light from a 635 nm CW diode laser injected from the bottom of the waveguide sample through an oil-immersion objective lens which also collects the output from the waveguides. The output is measured both on a calibrated photodetector as well as imaged in real-time. This setup allows measurement of the insertion loss of each device as well as capturing the output optical profile of the waveguides.

The fabrication resolution of the system under increasing laser powers is found by making air-suspended straight waveguides using a single pass of the laser (Fig. 2). These are supported between two larger cylindrical pillars of $\sim 4\ \mu\text{m}$ diameter (Figs. 2(a) and 2(b)). The lateral resolution found from the width of this suspended bar (measured in SEM images, Fig. 2(b)) is always 3-4 times smaller than the vertical resolution because of the typical shape of exposure voxels (Fig. 2(c)).⁸ The best lateral resolution of our system with the IP-L resist is 400 nm, although further optimisation has been discussed extensively in the literature.^{9,10} This resolution is expected due to the low repetition rate and longer pulses of the microchip system which leads to less precise energy transfer due to impact ionization effects.¹¹ For smaller powers, the resulting suspended beams are not structurally stable and break. The present direct write lithography thus produces waveguides which are weakly multimode, which are nevertheless sufficient to demonstrate the capability to straightforwardly create vertical arc waveguides. Further optimisation will produce single-mode waveguide circuits.

Arc waveguides in arrays with different arc geometry are fabricated on a single chip and tested. Arc diameters range from 10 to $50\ \mu\text{m}$ in $10\ \mu\text{m}$ steps and waveguide port diameters at the base of the arc range from 6 to $8\ \mu\text{m}$ (Figs. 3(a) and 3(b)). It is found that the geometry of the port where the arc is connected into the substrate can modify the input

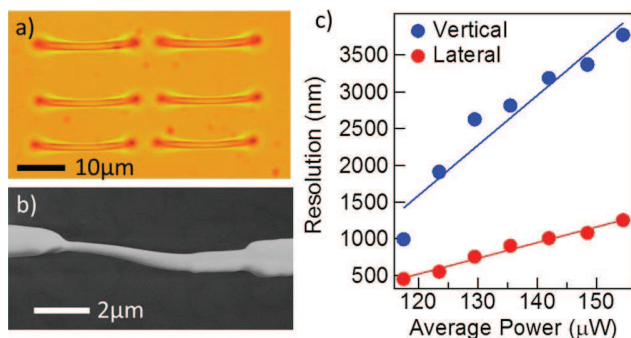


FIG. 2. (a) Optical image of an array of arc waveguides. (b) Typical fabricated suspended straight waveguide imaged from above in SEM. (c) Lateral and vertical dimensions of single-pass straight waveguides for increasing laser power, with 10 ms exposure time.

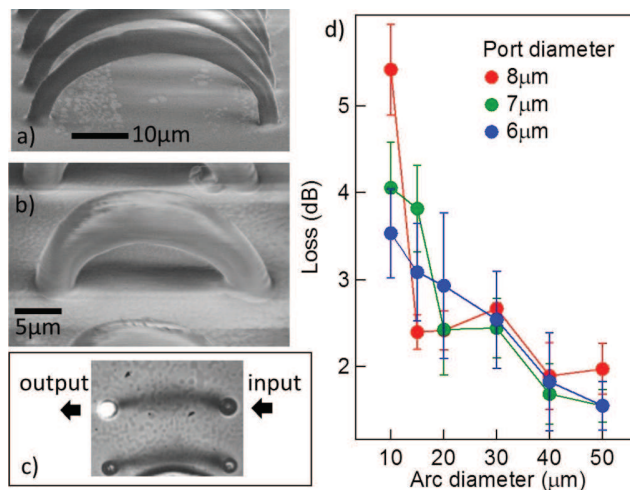


FIG. 3. (a) and (b) SEMs of vertical arc waveguides, with arc diameters of (a) $50\ \mu\text{m}$ and (b) $30\ \mu\text{m}$, and port diameters of (a) $2\ \mu\text{m}$ and (b) $6\ \mu\text{m}$. (c) Measurement image view through the laser input objective lens, indicating the input and (lit-up) output ports of the waveguide. (d) Insertion loss measurements of vertical arc waveguides of increasing arc and port diameters.

coupling and can be freely optimised with the 3D direct write fabrication strategy. Images in the measurement setup from the substrate side (Fig. 3(c)) show the arc waveguides and the coupling ports, with the output light spot clearly visible. Loss measurements (Fig. 3(d)) exhibit a general trend of increasing loss with smaller arc diameters. This is expected because of the higher radiation loss for smaller arc diameters with sharper bends. However, smaller arc diameters also mean shorter waveguides, which thus incur reduced propagation losses. Hence, these two effects counteract each other. Insertion losses are measured to be as low as 1.5 dB for waveguides with the largest arc diameters of $50\ \mu\text{m}$, and can be considerably improved in optimised designs (in progress). The loss is only sensitive to the port diameter for tighter arcs, due to the way different waveguide modes experience the total internal reflection inside the arc waveguide. The input/output coupling loss is not extracted here because of the difficulty in separating it from the overall propagation loss. This is because standard techniques such as the cut-back method¹² are not yet straightforwardly feasible for vertical arc waveguides. Similarly, Fabry-Perot techniques¹³ are also not available because of the low index contrast across the waveguide facet between IP-L and glass. The cross section of these arc waveguides is designed to be as circular as possible to make them polarization-insensitive; however, other waveguide cross-sectional shapes are certainly possible.

The obtained losses are in line with expectations from bend loss and roughness.¹⁴ Due to the capability to taper the entrance to such waveguides, coupling loss can be minimised in this approach. Single-mode waveguides are not yet possible but should be achieved with further optimisation of spatial dimensions and refractive contrast. This allows for various sensor designs including evanescent field and interferometric architectures.

To demonstrate this utility, we fabricate a variety of suspended splitters including the three-way and four-way devices of Fig. 4. By simply varying the angle between the arc

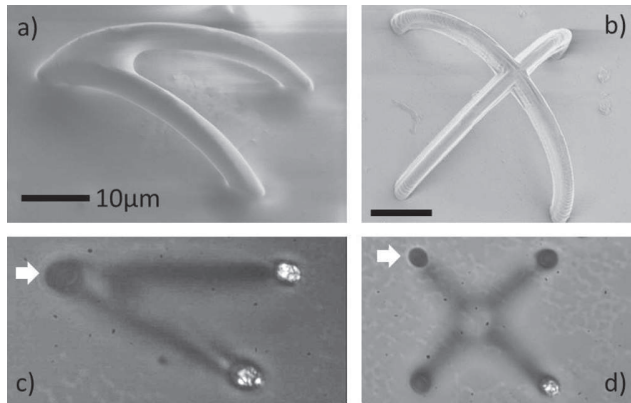


FIG. 4. (a) and (c) Three way and (b) and (d) four-way splitters produced from intersecting vertical arc waveguides. Scale bars are $10\ \mu\text{m}$. (c) and (d) Input ports marked with white arrows, producing output beams as imaged.

waveguide arms, a variable splitting ratio can be achieved, tuning from no cross-talk (Figs. 4(b) and 4(d)) to 50% coupling in each arm (Figs. 4(a) and 4(c)). Despite the multimode guidance, good performance is achieved in these devices showing that scattering from the directly written sidewalls is not a major problem nor the morphology at the intersection point. With such splitters and recombiners together with combinations of waveguides that pass under and over each other, a wide variety of 3D photonic circuits can be directly produced.

In summary, vertically standing arc waveguides are fabricated with two-photon polymerization using a low-cost picosecond laser. Directly written arc waveguides with various arc diameters and waveguide port diameters are demonstrated, with insertion loss down to 1.5 dB obtained. This provides the demonstration of an approach to waveguide

coupling into arrays and chips and is capable of further enhanced performance. Tight arcs possible with the refractive index contrast available allow complete sensors with individual footprints below $0.3\ \mu\text{m}^2$, enabling dense integration of sensor arrays. Such vertical standing arc waveguides can thus be useful as environmental sensors, offering alternative ways of input/output-coupling to planar waveguides, and providing an additional dimension to device integration for photonic integrated chips.

This work is supported by EPSRC Grant No. EP/G060649/1. C.W.L. gratefully acknowledges the support of A*STAR Singapore through the overseas postdoctoral sponsorships.

¹B. H. Cumpston, S. P. Ananthavel, S. Barlow, D. L. Dyer, and J. E. Ehrlich, *Nature (London)* **398**, 51 (1999).

²S. Kawata, H.-B. Sun, T. Tanaka, and K. Takada, *Nature (London)* **412**, 697 (2001).

³M. Deubel, G. Freymann, M. Wegener, S. Pereira, K. Busch, and C. M. Soukoulis, *Nature Mater.* **3**, 444 (2004).

⁴A. Ostendorf and B. N. Chichkov, *Photonics Spectra* **40**, 72 (2006).

⁵M. Farsari and B. N. Chichkov, *Nat. Photonics* **4**, 450 (2009).

⁶H. Ma, A. K.-Y. Jen, and L. R. Dalton, *Adv. Mater.* **14**, 1339 (2002).

⁷R. Woods, S. Feldbacher, G. Langer, V. Satzinger, V. Schmidt, and W. Kern, *Polymer* **52**, 3031 (2011).

⁸H.-B. Sun, M. Maeda, K. Takada, J. W. M. Chon, M. Gu, and S. Kawata, *Appl. Phys. Lett.* **83**, 1104 (2003).

⁹Ch. J. Schwarz, A. V. V. Nampoothiri, J. C. Jasapara, W. Rudolph, and S. R. J. Brueck, *J. Vac. Sci. Technol. B* **19**, 2362 (2001).

¹⁰K. Takada, H.-B. Sun, and S. Kawata, *Appl. Phys. Lett.* **86**, 071122 (2005).

¹¹M. Malinauskas, P. Danilevicius, and S. Juodkazis, *Opt. Express* **19**, 5602 (2011).

¹²R. G. Hunsperger, *Integrated Optics: Theory and Technology* (Springer Verlag, New York, 1991), p. 83.

¹³T. Feuchter and C. Thirstrup, *IEEE Photonics Technol. Lett.* **6**, 1244 (1994).

¹⁴K. S. Kaufman, R. Terras, and R. F. Mathis, *J. Opt. Soc. Am.* **71**, 1513 (1981).